Mem. S.A.It. Vol. 82, 489

Memorie della

Measuring turbulence in clusters with XMM-Newton RGS

J.S. Sanders

Institute of Astronomy, Madingley Road, Cambridge, CB3 0HA, UK
e-mail: jss@ast.cam.ac.uk

Abstract. We describe how the reflection grating spectrometers on the XMM-Newton observatory can be used to place limits on the amount of turbulence in the intracluster medium in galaxy clusters, groups and elliptical galaxies. We find a limit on gas motions in the center of Abell 1835 of less than 274 km s^{-1} , equivalent to an upper limit of 13% of the thermal energy density. Although we are limited to only examining fairly relaxed, point-like objects, we find little evidence for strong gas motions in a sample of 62 objects. After modeling and subtraction of the broadening due to the extent of the sources, we find five targets with a limit of less than 200 km s^{-1} . There is some evidence for additional motions in two of the sample, Klemola 44 and RXJ 1347.5-1145.

Key words. Intergalactic medium — X-rays: galaxies: clusters

1. Introduction

Simulations of galaxy clusters in the context of structure formation predict that there should be substantial turbulence in the intracluster medium (ICM) of galaxy clusters (e.g. Vazza et al. 2009; Lau et al. 2009). In relaxed objects, the predicted level of energy in turbulence relative to the thermal energy rises from $\sim$ 5% in the cores to 20% in the outskirts. In addition, there is widespread active galactic nuclei (AGN) feedback in galaxy clusters by the injection of jets and cavities (see review of McNamara & Nulsen 2007). This feedback should induce motions at the level of ~ 250 km s^{-1} (Brüggen et al. 2005). Observationally we observe weak shocks (Fabian et al. 2006; Forman et al. 2007) and sound waves in clusters (Fabian et al. 2006; Sanders & Fabian 2008).

There have been several indirect measurements of the amount of turbulence in cluster cores. In the center of clusters or groups the ICM can be optically thick in the light of resonance lines. If there are gas motions the optical depth is reduced. Therefore if resonance scattering is observed, this puts an upper limit on motions. In NGC 4636, Xu et al. (2002) put upper limits on the turbulent velocity dispersion of less than 10% of the sound speed. Werner et al. (2009) also found a maximum of 5% of energy is in turbulent motions. However, in the Perseus cluster Churazov et al. (2004) found a lack of scattering, implying velocities of at least half the sound speed. If there are such velocities, they must maintain the straight morphology of the Hα nebula in Perseus on scales of 10s of kpc (Fabian et al. 2003).

The contribution of non-thermal pressure has also been examined by comparing optical and X-ray gravitational profiles in M87 and

Send offprint requests to: J.S. Sanders

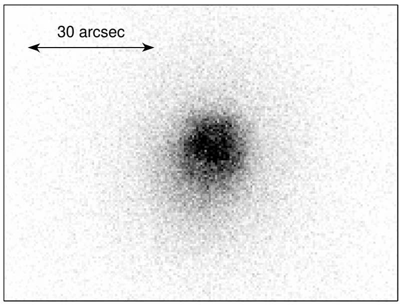

Fig. 1. Chandra X-ray image of Abell 1835. The X-ray emission of the cool gas is concentrated into a small region on the sky.

NGC 1399 (Churazov et al. 2008), and found to be less than 10% of the thermal gas pressure.

Schuecker et al. (2004), however, put a minimum level of 10% of the total pressure in turbulence in the Coma cluster, by examining the spectrum of the variations in a pressure map. This object is likely to be a disturbed system, and would be expected to have relatively high levels of turbulence.

Previously, there have been no direct measurements on the amount of turbulence in the ICM. The shape of X-ray lines can be used to determine the velocity structure (Inogamov & Sunyaev 2003). Unfortunately the spectral resolution of CCD instruments is too low to do this. We decided in investigate whether it was possible to use the Reflection Grating Spectrometers (RGS) on XMM-Newton to make useful constraints on turbulence in galaxy clusters.

As the RGS are slitless spectrometers, the spectral resolution depends on the extent of the source on the sky. The emission lines are broadened by $\Delta\lambda \approx (0.124/m)\Delta\theta$ Å, where m is the spectral order and $\Delta\theta$ is the half energy width of the source in arcmin (Brinkman et al. 1998). Therefore to get the best spectral resolution, point-like objects are required.

2. Abell 1835

We observed Abell 1835 ($z = 0.2523$) for a total of 254 ks using XMM-Newton. We describe our analysis fully in Sanders et al. (2010). Abell 1835 is a very good source for measuring line widths because it is an object that was a good candidate for hosting a cooling flow: it is compact (Fig. 1), luminous ($\sim 2\times10^{45}$ erg s^{-1}) and contains cool X-ray emitting gas in its core.

We processed the data files for our observations with SAS 9.0 and combined them together using RGSCOMBINE. A background was obtained from the observation at large cross-dispersion angles. The fluxed, background-subtracted, combined spectrum is shown in Fig. 2. The spectrum shows narrow Fe-L emission lines, demonstrating that the emission comes from a small region on the sky and there is no obvious velocity broadening.

We fitted the first and second order combined spectra in XSPEC 12.5.1 by minimizing the modified C-statistic. The lines in the spectral model were broadened by the thermal line width plus an additional line-of-sight velocity added in quadrature. The abundances of elements with strong lines in the spectral region examined (7 to 28Å or 16Å for the 1st and 2nd orders, respectively) were free in the fit and the other elements were tied to the Fe abundance. We used the SPEX version 2.00.11 model, obtaining a best fitting temperature of 3.67 ± 0.16 keV. If another temperature component is added to the model it is not strongly required and has a temperature ~ 0.6 keV.

The best-fitting additional line width is zero. In Fig. 3 we show the fit statistic changes with increasing line width. For the normal fit ('without RGSXSRC'), we obtain an upper limit at the 90% confidence level on the additional line-of-sight broadening of 274 km s^{-1}. This value includes both the turbulent broadening plus any contribution from the fact that source is extended.

We can use the RGSXSRC model to try to take account of the line broadening caused by the spatial extent of the source. This model uses an X-ray image of the source to calculate the broadening, but makes the major assumption that the spectrum of the source is position-independent. Using this model we obtain an upper limit of 182 km s^{-1}.

This limit on the velocity can be converted to an upper limit on the fraction of the thermal

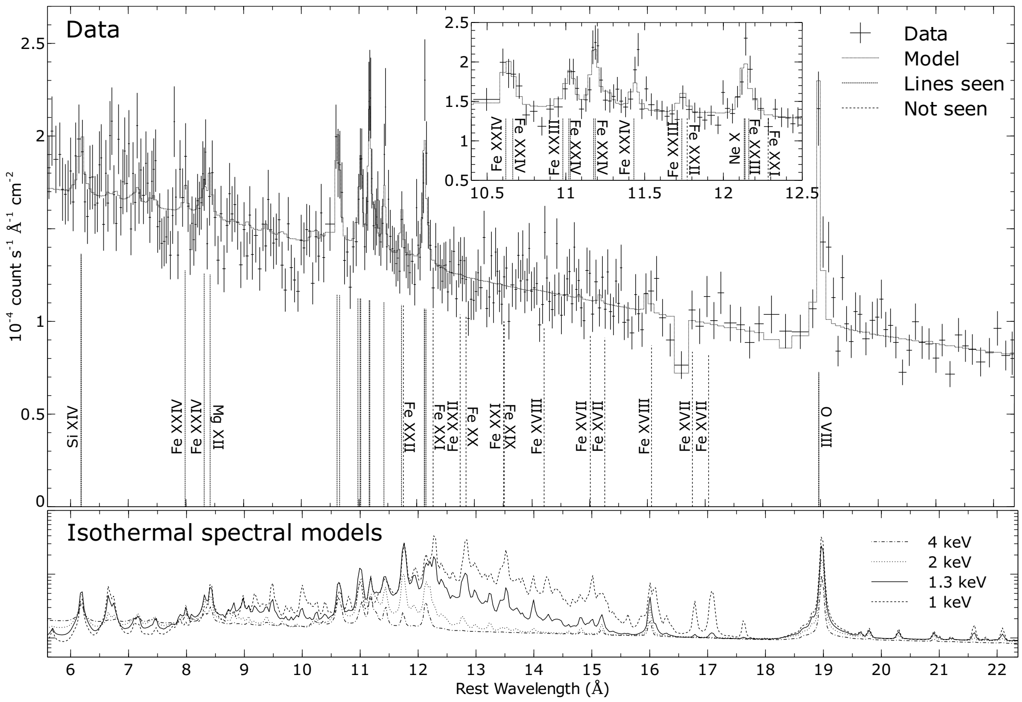

Fig. 2. RGS spectrum of Abell 1835. The top panel shows the fluxed spectrum plus a zoom on the Fe-L region. Also listed are the observed and unobserved emission lines. The bottom panel shows model thermal spectra at different temperatures.

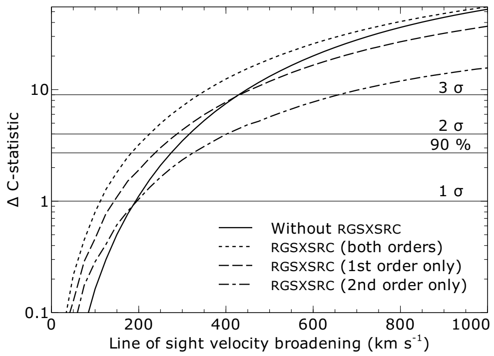

Fig. 3. Upper limits on the line broadening of the Abell 1835 spectrum. Shown are the results with and without modeling the broadening caused by the extent of the source.

energy in the form of turbulence, using equation 11 in Werner et al. (2009), $V_{\rm los}^2\,\mu m_{\rm p}/kT$, where $V_{\rm los}$ is our measured line-of-sight velocity, μ is the mean particle mass, $m_{\rm p}$ is the proton mass and kT is the temperature. From our most conservative upper limit on the velocity, this implies an upper limit of 13% of the thermal energy density in turbulent energy density.

3. Larger sample

We decided to see whether we could obtain additional limits for a larger sample of objects. In Sanders et al. (2011) we examined a sample of 62 clusters, groups and ellipticals. To generate this sample we examined the XMM-Newton archive to find observations of clusters, groups and ellipticals with obvious RGS line emission. The sample is therefore not statistically complete or rigorous and is biased towards bright relaxed objects with cool cores.

For these observations we automated the download, processing and fitting of the spectra, and the combination of multiple obser-

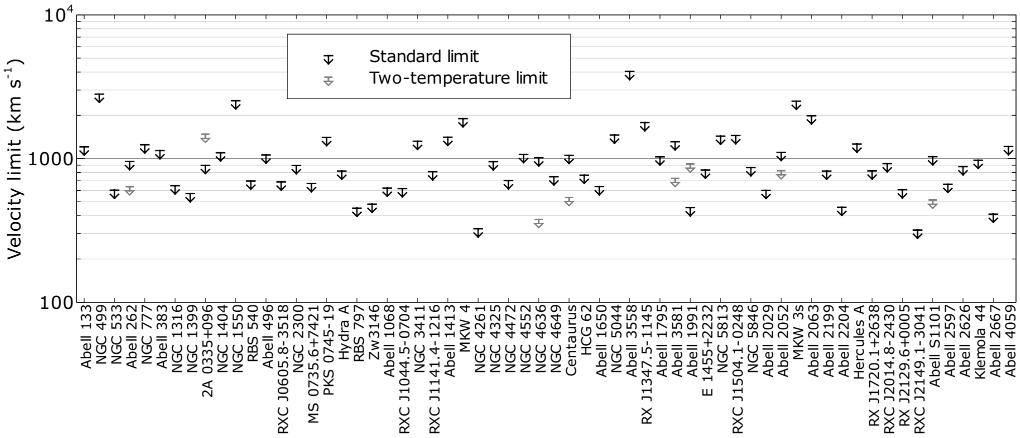

Fig. 4. Upper limits at the 90% level on the broadening for the sample of clusters. Some targets have been fitted with models using two temperature components.

vations of the same targets. The spectra for the targets were fit in a similar way to the Abell 1835 data, using a background extracted locally from each dataset. The spectra were fit with the APEC 1.3.1 spectral model (Smith et al. 2001). We obtained best fitting line broadening, temperatures, metallicities, emission measures and Galactic absorbing column densities. We used a second thermal component when the fits were significantly improved by its addition. Some datasets were extremely line-rich and showed little continua. For those we fixed the Fe metallicity to the solar value in order to constrain the ratio of the other elements to Fe.

We show in Fig. 4 the upper limits on the broadening for our sample of objects. These limits were calculated by varying the broadening in order to give a change in fit statistic of 2.71. We tested this method using Markov Chain Monte Carlo (MCMC) in XSPEC to calculate the probability of the parameter values given the data.

We find five objects with limits on the broadening of less than 500 km s^{-1}. Unfortunately none of the targets improve on the limit for Abell 1835. There are an additional two targets below 500 km s^{-1} when two temperature components are used. Half of the targets have a limit of less than 700 km s^{-1}, although our sample is biased to relaxed objects.

Shown in the top panel of Fig. 5 are the limits we obtain as a function of the temperature of the object from the spectral fit to the RGS spectrum (which is weighted towards the center of the source). Note that this plot should not be used to infer the distribution of velocities as a function of temperature as our sample is biased. We also include on this plot lines of constant fractions of turbulent to thermal energy density.

We decided to subtract the contribution to the line width from the spatial extents of the sources. Rather than use a model such as RGSXSRC which assumes that the spectrum of the source is position-independent, we modeled source spectra using Chandra imaging spectroscopy results, and subtracted this contribution from the values measured from the real spectra.

For this analysis, we created Chandra temperature, metallicity and emission measure maps for around half the objects in the sample. We developed an automated Chandra spectral mapping tool. The Contour Binning algorithm (Sanders 2006) selected regions with similar surface brightness containing a minimum signal to noise ratio. Spectra were extracted from these regions. The spectra were fit with an APEC model assuming solar relative abundances.

We took these maps and simulated deep exposures for each spatial bin. The RGSRMFGEN

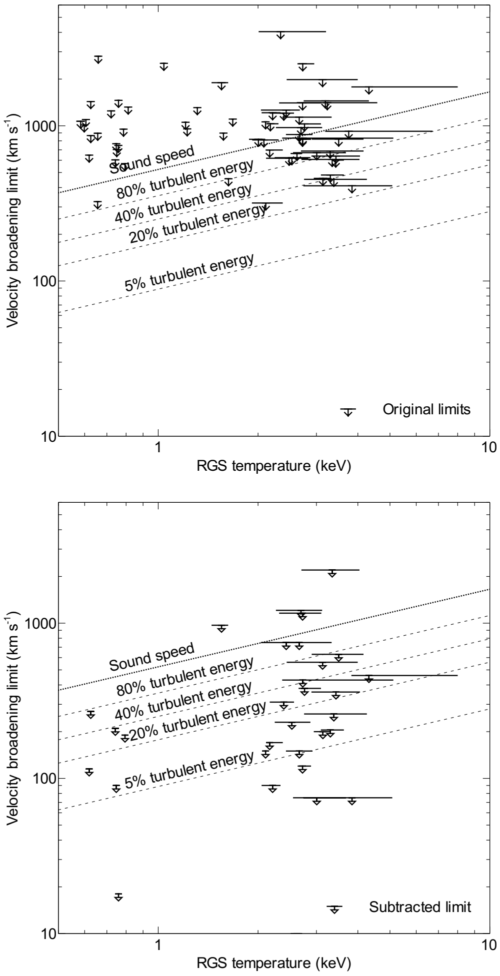

Fig. 5. 90% confidence level limits for our sample as a function of RGS temperature, before (top) and after (bottom) subtraction of the contribution from the spatial extent. We add a $50\,\mathrm{km\,s^{-1}}$ systematic to the limits for the subtracted data points.

program was used to create a response matrix given the distribution of the bin in terms of the dispersion direction. We then used XSPEC to simulate the spectra for that bin, assuming solar relative abundances. The spectra were then added for all the bins (repeating the simulations for both RGS instruments, and using an exposure time 100 times greater than the real exposure times).

The bottom panel of Fig. 5 shows the effect of subtracting the line widths measured from the simulated spectra. We add an additional $50\,\mathrm{km\,s^{-1}}$ systematic uncertainty due to the calibration uncertainty of the line spread functions of the RGS instruments. We find six targets with less turbulence than 5% of the thermal energy. The clusters Zw3146, A496, A1795, A2204 and HCG62 show broadening of less than $200\,\mathrm{km\,s^{-1}}$.

We found two objects with evidence for broadening: Klemola 44 and RX J1347.5-1145. The broadening for Klemola 44 is $1300\,\mathrm{km\,s^{-1}}$ (3.6% probability of occurring by chance), and $840\,\mathrm{km\,s^{-1}}$ (with a 6% probability of chance). The significance of the results improve if a MCMC analysis is done. Both of these objects are likely to be unrelaxed. Klemola 44 has a disturbed morphology and lacks a strong central peak or cool core. It also has different populations of velocity in the galaxies (Green et al. 1990). RX J1347.5-1145 is likely to have recently undergone a merger (e.g. Allen et al. 2002), as seen from a hot region near the core of the cluster.

4. Future work

Some targets in our sample show redshifts which are substantially different from the optical redshift of the source. It will be interesting to see whether there is any other evidence for bulk flows in these objects.

As our best limits are obtained for the most point-like cool-core targets, we have proposed XMM should observe a sample of clusters chosen to be spatially compact, bright, and have cool X-ray emitting gas in their cores. We have obtained time on four of these targets. An analysis of the data from one of these targets, MACS 2229 (Fig. 6), shows a limit on the broadening of $280\,\mathrm{km\,s^{-1}}$, without any subtraction of the spatial broadening component.

Our modeling of the spatial broadening is relatively simplistic. We do not take account of the uncertainty in the distribution of the ICM properties from the Chandra mapping. A MCMC analysis (e.g. Peterson et al. 2007)

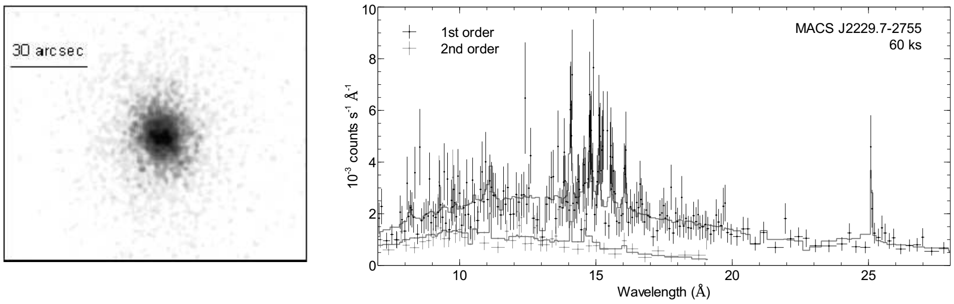

Fig. 6. Chandra X-ray image of MACS J2229.7-2755 (left) and 60 ks RGS spectrum from our current program of observations (right).

could take account of these uncertainties. In addition, improvements to the RGS line spread function calibration would reduce the uncertainties in the analysis.

The launch of the ASTRO-H observatory in 2014, with its spectral resolution of at least 7 eV, promises exciting results. It will be able to probe the velocity structure in the Fe-K lines over a much wider range of targets than we have been able to examine.

5. Conclusions

We have shown that the XMM RGS instruments can provide useful limits or even measurements of the amount of turbulence in the cores of fairly relaxed clusters. For all but two of the clusters examined we find no evidence for strong turbulence.

Acknowledgements. I thank Andy Fabian, Randall Smith and John Peterson for their contributions to the original work this paper reports upon.

References

Allen, S. W., Schmidt, R. W., & Fabian, A. C. 2002, MNRAS, 335, 256
Brinkman, A., et al. 1998, in Proceedings of the First XMM Workshop on Science with XMM, http://xmm.esac.esa.int/
Brüggen, M., Hoeft, M., & Ruszkowski, M. 2005, ApJ, 628, 153
Churazov, E., Forman, W., Jones, C., Sunyaev, R., & Böhringer, H. 2004, MNRAS, 347, 29
Churazov, E., et al. 2008, MNRAS, 388, 1062
Fabian, A. C., et al. 2003, MNRAS, 344, L48
Fabian, A. C., et al. 2006, MNRAS, 366, 417
Forman, W., et al. 2007, ApJ, 665, 1057
Green, M. R., Godwin, J. G., & Peach, J. V. 1990, MNRAS, 243, 159
Inogamov, N. A. & Sunyaev, R. A. 2003, Astronomy Letters, 29, 791
Lau, E. T., Kravtsov, A. V., & Nagai, D. 2009, ApJ, 705, 1129
McNamara, B. R. & Nulsen, P. E. J. 2007, ARA&A, 45, 117
Peterson, J. R., Marshall, P. J., & Andersson, K. 2007, ApJ, 655, 109
Sanders, J. S. 2006, MNRAS, 371, 829
Sanders, J. S. & Fabian, A. C. 2008, MNRAS, 390, L93
Sanders, J. S., Fabian, A. C., & Smith, R. K. 2011, MNRAS, 410, 1797
Sanders, J. S., Fabian, A. C., Smith, R. K., & Peterson, J. R. 2010, MNRAS, 402, L11
Schuecker, P., et al. 2004, A&A, 426, 387
Smith, R. K., Brickhouse, N. S., Liedahl, D. A., & Raymond, J. C. 2001, ApJ, 556, L91
Vazza, F., et al. 2009, A&A, 504, 33
Werner, N., et al. 2009, MNRAS, 398, 23
Xu, H., et al. 2002, ApJ, 579, 600